A typical slow reaction $H(^2S)+S_2(X^3\Sigma_g^-)\rightarrow SH(X^2\Pi)+S(^3P)$ on a new surface: Quantum dynamics calculations*

Wei Wei(魏 巍)[a], Gao Shou-Bao(高守宝)[a], Sun Zhao-Peng(孙兆鹏)[b], Song Yu-Zhi(宋玉志)[a], and Meng Qing-Tian(孟庆田)[a]†

[a] College of Physics and Electronics, Shandong Normal University, Jinan 250014, China
[b] School of Physics, Shandong University, Jinan 250014, China

(Received 6 December 2013; revised manuscript received 10 January 2014; published online 28 May 2014)

Quantum dynamics calculations for the title reaction $H(^2S)+S_2(X^3\Sigma_g^-)\rightarrow SH(X^2\Pi)+S(^3P)$ are performed by using a globally accurate double many-body expansion potential energy surface [*J. Phys. Chem. A* **115** 5274 (2011)]. The Chebyshev real wave packet propagation method is employed to obtain the dynamical information, such as reaction probability, initial state-specified integral cross section, and thermal rate constant. It is found not only that there is a reaction threshold near 0.7 eV in both reaction probabilities and integral cross section curves, but also that both the probability and cross section increase firstly and then decrease as the collision energy increases. The existence of the resonance structure in both the probability and cross section curves is ascribed to the deep potential well. The calculation of the rate constant reveals that the reaction occurring on the potential energy surface of the ground-state HS_2 is slow to take place.

Keywords: quantum dynamics, Chebyshev real wave packet propagation, $H+S_2$

PACS: 31.15.xv, 34.50.−s, 03.67.Lx **DOI:** 10.1088/1674-1056/23/7/073101

1. Introduction

As one of the major sulfur-bearing species existing in the atmosphere of large planets,[1–3] hydrogen sulfide (HS_2) plays an important role in combustion and atmospheric chemistry.[4–6] However, because most researchers concentrate their attention on the structural and spectroscopic properties of HS_2 radical, much less attention has been paid to its dynamics calculations than its controversial isovalent counterparts HSO[7] or HO_2.[8,9] In 1950, Porter[10] first detected HS_2 radical during the flash photolysis of H_2S_2. Since it was found that the oxidation of HS_2 radical can produce SH radicals which can form H_2S_2 in the atmosphere,[11] more and more researchers started to focus on the HS_2 radical. In the analysis of electron structures, it is found that the HS_2 radical has two states, i.e., the ground-state HS_2 (X^2A'') and the excited state HS_2 (A^2A'). The ground state of HS_2 radical has been well characterized by spectroscopy in the microwave region,[12] far-infrared laser magnetic resonance spectroscopy,[13] as well as spectroscopy in the millimeter wave region.[14] However, due to the low mass separation, HS_2 could only be measured in a mixture with S_2.[15] In this case, the first excited state, located at 7254 cm^{-1} above the ground state was not observed.[16] In 2008, Peterson *et al.*[17] reported a theoretical study of the spectroscopic properties of the ground and first excited electronic states of HS_2. Subsequently, Michaela and Ulrich[15] studied the photodetachment–photoelectron spectroscopy of disulfamide for the same state. However, there has been little experimental or theoretical study on the S+SH and H+S_2 reaction. For the convenience of discussion, we draw a parallel between HS_2 and HO_2 radical, in which O and S are the elements of the same group. Comparison of their potential energy surfaces (PESs)[9,18] shows that the relevant reactions may have similar dynamic properties due to the similar characteristics, such as being barrierless with a deep well. Therefore, there is a great development space in the quantum scattering dynamical studies of the endoergic reaction between the hydrogen atom and the sulfur molecule.

Recently, employing the double many-body expansion (DMBE) theory, Song and Varandas[19] constructed an accurate global PES for the ground-state $HS_2(X^2A'')$, and the obtained information has been proven to agree well with the experimental and other theoretical values. As described in Fig. 1, the deep well in HS_2 PES corresponds to the stable radical HS_2 (X^2A''), which can support some bound states and resonances. The energies relative to the minimum of the PES for $H+S_2$ and S + SH are predicted to be 2.6 eV and 3.3 eV, respectively. Obviously, there is an energy difference of about 0.7 eV between reactant and product.

Just as in other chemical systems where the non-adiabatic effect plays an important role,[20] for reaction $H+S_2(X^3\Sigma_g^-)$, the ^3P state of the S atom crosses ^1D state in the reactant arrangements, and the existence of the spin-orbit coupling makes it a challenge to obtain accurate dynamics information without dynamic approximation. However, nonadiabatic calculations are beyond our scope, since the reaction $H(^2S)+S_2(X^3\Sigma_g^-)\rightarrow SH(X^2\Pi)+S(^3P)$ studied here is

*Project supported by the National Natural Science Foundation of China (Grant Nos. 11074151 and 11304185).
†Corresponding author. E-mail: qtmeng@sdnu.edu.cn
© 2014 Chinese Physical Society and IOP Publishing Ltd

based on the single-sheeted PES introduced above. The time-dependent (TD) quantum method,[21,22] which is proved to have a higher computational efficiency than time-independent (TI) quantum method, is used to calculate the related reaction dynamics. In this method, the wave packet is propagated in the Chebyshev order domain. Compared with the conventional time wave packet approach,[23,24] the present method is accurate and efficient because no approximation of the propagator is needed when the wave packet propagates in real space.[25] Moreover, it can also propagate the wave packet exactly for dealing with complex-forming reaction.[26] Using this method, Sun *et al.*[27,28] studied the reaction dynamics of $O(^1D)+D_2\rightarrow OD+D$ and $C(^1D)+H_2(D_2)\rightarrow CH(D)+H(D)$ in 2011 and 2013, respectively, while Ma and Guo *et al.*[9] investigated the $H(^2S)+O_2(\tilde{a}^1\Delta_g)\rightarrow O(^3P)+OH(X^2\Pi)$ reaction in 2011. The excellent agreement between the theoretical prediction and experimental results shows that the TD Chebyshev propagation method is highly effective.

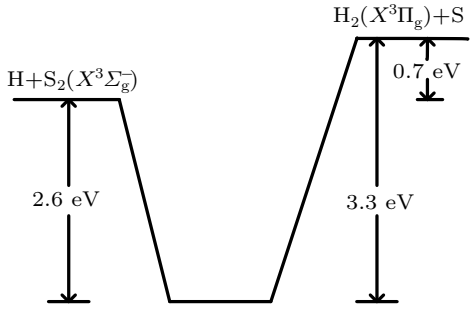


Fig. 1. Schematic PES for the $H+S_2(X^3\Sigma_g^-)\rightarrow SH(X^2\Pi)+S$ reaction.

In the present TD calculation, the dynamical information reflecting the reaction features on the adiabatic PES for HS_2 (X^2A'') involves the reaction probabilities, integral cross sections (ICSs), the rate constants, etc. The paper is organized as follows. In Section 2, we present the Hamiltonian of the system and the Chebyshev wave packet propagation method, with the mathematical expressions for reaction probability and the initial state-specified ICS. In Section 3, the exact quantum dynamical results are provided and discussed. Meanwhile, the feature of the reaction probabilities, ICS and rate constant curves are analyzed. Finally, we conclude the results in Section 4.

2. Theory

The quantum dynamical calculations are carried out in the reactant Jacobi coordinates (R,r,γ), in which the variables indicate the distance between H and S–S center of mass, the reactant S–S distance, and the angle enclosed by R and r, respectively. With the reactant coordinates, the Hamiltonian of the system can be written as ($\hbar=1$)

$$\hat{H}=-\frac{1}{2\mu_R}\frac{\partial^2}{\partial R^2}-\frac{1}{2\mu_r}\frac{\partial^2}{\partial r^2}+\frac{(\hat{J}-\hat{j})^2}{2\mu_R R^2}+\frac{\hat{j}^2}{2\mu_r r^2}+V(R,r,\gamma), \tag{1}$$

where $\mu_r=m_S m_S/(m_S+m_S)$ and $\mu_R=m_H(m_S+m_S)/(m_S+m_S+m_H)$ are the reduced masses, $\hat{j}$ the rotational angular momentum operators of the diatomic molecule (S_2), $\hat{J}$ the total angular momentum, $V(R,r,\gamma)$ the potential energy of the ground-state HS_2 (X^2A''). For a total angular momentum J, the squared orbital angular momentum operator can be expressed as follows:

$$(\hat{J}-\hat{j})^2=\hat{J}^2+\hat{j}^2-2\hat{J}_z\hat{j}_z-\hat{J}_+\hat{j}_--\hat{J}_-\hat{j}_+, \tag{2}$$

where $\hat{J}_z$ and $\hat{j}_z$ are projections of $\hat{J}$ and $\hat{j}$ onto the body-fixed z axis, respectively, and $\hat{J}_+(\hat{J}_-)$ and $\hat{j}_+(\hat{j}_-)$ are the corresponding raising (lowing) operators, which are responsible for the Coriolis coupling.[29]

In our work, the initial wave packet is propagated by the modified Chebyshev recursion[30]

$$|\psi_{n+1}\rangle=D(2\hat{H}_{\text{scaled}}|\psi_n\rangle-D|\psi_{n-1}\rangle), \tag{3}$$

with $|\psi_1\rangle=D\hat{H}_{\text{scaled}}|\psi_0\rangle$ and $|\psi_0\rangle$ being the initial wave packets which can be defined in the space-fixed (SF) frame as follows:[25]

$$|\psi^{J_p}_{v_i j_i l_i}\rangle=N\mathrm{e}^{-(R-R_{i0})^2/2\sigma^2}\cos(k_{i0}R)\phi_{v_i j_i}(r)|j_i l_i,J_p\rangle, \tag{4}$$

where N is the normalization constant, k_{i0}, R_{i0}, and σ are the central momentum, the central position, and width, respectively, $\phi_{v_i j_i}(r)$ is the rovibrational eigenfunction of the S_2 reactant, v_i, j_i, and l_i are the vibrational, rotational, and initial orbital angular momentum quantum numbers, respectively.

In order to avoid divergence, the actions of the scaled Hamiltonian onto the Chebyshev wave packet are calculated using a pseudo-spectral method.[31] The damping function, which is used to prevent the artificial reflection at the grid edges, is defined as

$$D(R)=\begin{cases}1, & R\le R_d,\\ \mathrm{e}^{-d_R(R-R_d)^2}, & R>R_d,\end{cases} \tag{5}$$

where R_d is the onset of the damping and d_R controls the extent of the damping. By projecting the Chebyshev wave packet onto a set of product state specific wave packets, one can obtain the Chebyshev correlation functions[32] C_k^{fi} as

$$C_k^{fi}=\left\langle\phi_{v_f j_f}\right|\left\langle j_f l_f,J_P|\psi_k(R'=R'_\infty)\right\rangle, \tag{6}$$

through which the S-matrix elements, the significant quantities for giving the related dynamical information, can also be obtained.

Using the S-matrix elements, the total reaction probability can be expressed by the final-state-sum as[33]

$$P(E)=\sum_{J_p l_i f_i}\left|S^{J_p}_{v_f j_f l_f, v_i j_i l_i}(E)\right|^2=\frac{1}{\pi\mu_r\left|a_i(E)\right|^2(E_{max}-E_{min})^2\sin^2\theta}\mathrm{Im}\left\langle\sum_k(2-\delta_{k0})\,\mathrm{e}^{-\mathrm{i}k\theta}\psi_k\sum_{k'}(2-\delta_{k'0})\,\mathrm{e}^{-\mathrm{i}k'\theta}\left[\delta(r-r_f)\frac{\partial}{\partial r}\psi_{k'}\right]\right\rangle, \quad (7)$$

where $r=r_f$ defines the dividing surface which is the position of the calculated flux, and θ is the Chebyshev angle.

By assembling the initial state-specified reaction probabilities for various J, the cross section can be given by

$$\sigma_{v_i j_i}(E_c)=\frac{\pi}{(2j_i+1)k_i^2}\sum_{J,p,\Omega\le\min(J,j_i)}(2\hat{J}+1)P^{J_p}_{v_i j_i\Omega}(E_c), \quad (8)$$

where $k_i=\sqrt{2\mu_R E_c}$ with E_c being the collision energy. Through averaging the corresponding ICS over the collision energy, the initial state-specified rate constant can be derived by

$$k_{v_i j_i}(T)=\frac{f}{k_B T}\left(\frac{8}{\pi\mu_R k_B T}\right)^{1/2}\int_0^\infty\sigma_{v_i j_i}(E_c)\,\mathrm{e}^{-E_c/k_B T}E_c\,\mathrm{d}E_c, \quad (9)$$

where k_B is the Boltzmann constant, T the temperature, and f the electronic degeneracy factor for the total reaction,[34] which is obtained by the electronic partition function[19]

$$Q_{el}=[5+3\exp(-569.83/T)+\exp(-825.34/T)]\times[1+\exp(-542.36/T)]. \quad (10)$$

3. Results and discussion

3.1. Numerical parameters

The relevant numerical parameters used in our calculations with respect to the $J=0$ reaction probability are summarized in Table 1. Since sulfur is an atom with large mass, more basis functions, grid points or propagation steps should be used than those of $H+O_2$.[19] In order to converge ICS up to the collision energy of 1.6 eV, 46 partial waves are needed for $H+S_2$ calculations.

Table 1. Numerical parameters used in the wave packet calculation (in atomic units).

Parameter	Value
Grid/basis ranges and sizes	$R\in(0.1,21.0)$, $(N_R=120)$
	$r\in(0.5,21.0)$, $(N_r=400)$
	$\gamma\in(0,90)$, $(N_\gamma=45)$
Absorption potential	$R_d=11.0$, $d_R=0.05$
	$r_d=13.0$, $d_r=0.01$
Initial wave packet	$R_0=10.0$, $E_0=0.8$ eV, $\delta=0.3$
Spectral control	Energy cut of 0.5 Hartree
Position of the flux calculated	$r_f=13$
Propagation steps	10000

3.2. Reaction probabilities

The total reaction probabilities of $H+S_2$ for two partial waves ($J=0$, $J=20$) in the energy range from 0.7 to 1.6 eV are compared in Fig. 2. Although there is no barrier along the minimum energy path in the entrance channel, it can be seen from the figure that the reaction probabilities for $J=0$ are quite small (less than 1.6% in Fig. 2). The phenomenon is very similar to the result which was obtained from the $H+O_2$ reaction in Ref. [35], since oxygen and sulfur belong to the oxygen group elements with similar chemical properties. Some studies showed that this phenomenon is due to the fact that the system does not seem to follow the reaction path and produces very little product.[35] However, as it can be seen in Fig. 2, due to the influence of centrifugal potential, the reaction probabilities for $J=0$ are much larger than the result obtained for J (take case of the reaction probabilities for $J=20$).

As shown in Fig. 1, the energy of the product is higher than that of the reactant, i.e., this is an endothermic reaction with a well, and the energy difference between reactant and product is 0.7 eV. This energy difference is just the threshold energy in the curve of reaction probability versus collision energy for $J=0$, as shown in Fig. 2. Because of the centrifugal potential associated with $\hat{J}$, the threshold moves to a higher energy as the total quantum numbers J increases. In addition, as shown by the dash-dotted line in Fig. 2, with the increase in the collision energy, by and large, the reaction probability begins to increase and then decreases when the collision energy is greater than 1.5 eV. The former case is understandable since, in general, the increase in collision energy may help to overcome the threshold energy and enhance the reaction probability, but when the collision energy is large enough, the opportunities of reactants taking part in reaction decrease with increasing the energy, which is the reason for the latter case. Meanwhile, because of the deep potential well, the reaction probability curves show distinct resonance structures in all range, and the sharp resonance peaks also indicate the existence of the long lifetime of the participating resonances.

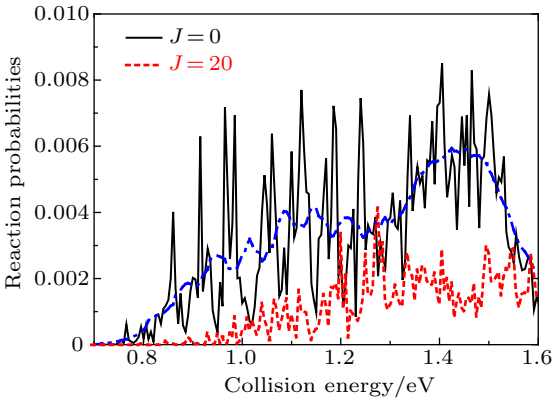


Fig. 2. (color online) Total reaction probabilities for the $H+S_2(X^3\Sigma_g^-, v=0, j=0)$ reaction for two J values.

If the reactant molecule S_2 is in the vibrational excited state ($v = 1$, $j = 0$), the reaction dynamics will display a significant change. The comparison of reaction probabilities for two vibrational quantum numbers ($v = 0, 1$) (shown in Fig. 3) shows that the reaction for $v = 1$ is more reactive and the threshold of the reaction shifts to lower collision energies with the increase in the S_2 vibrational quantum number, which suggests that the raising of vibrational quantum number is propitious to the reaction.

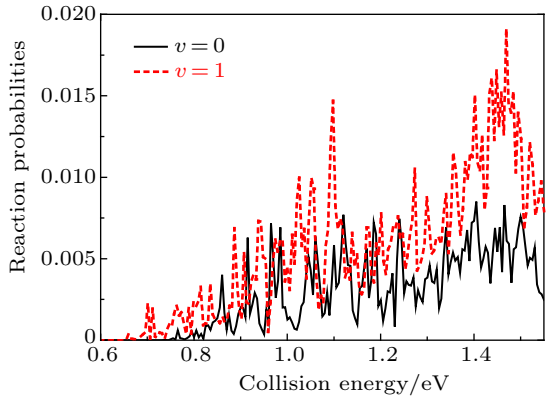


Fig. 3. (color online) Total reaction probabilities for the H + $S_2(X^3\Sigma_g^-, v, j = 0)$ reaction with $J = 0$ for two v values.

3.3. Total integral cross sections

In order to provide more plentiful dynamics information, we give the total reaction sections at the collision energy ranges of 0.7–1.6 eV from $J = 0$ to $J = 46$ as depicted in Fig. 4. Obviously, because of the sum of all partial waves, the ICS shows an increase-then-decrease trend which is more obvious than the feature of the probability curves. The reason for this is the same as the related explanation for the changing probability with the collision energy. Meanwhile, there are clear threshold energy near $E_c = 0.7$ eV and residual oscillations because of the existence of the well. Despite the fact that the ICS sums the weighted reaction probabilities over many partial waves, the small oscillations illustrate that the partial wave sum cannot wash away all the resonance features which completely resemble the resonance features of the reaction probabilities.[36] It is obvious from the curves that, the overall reactivity is not high, with ICS being less than 0.016 Å^2 in this energy region for $v = 0$. This feature is quite analogous to the ICS curves of the H + O_2 reaction.[18]

Also illustrated in Fig. 4 is the effect of the reagent vibrational excitation. It can be seen that with the increase in the vibrational quantum number, the ICS has a marked increase. Considering that the ICS is the sum of the weighted reaction probabilities over many partial waves, and the increase in the vibrational quantum number is in favor of the increase in the reaction probability, this is a natural result.

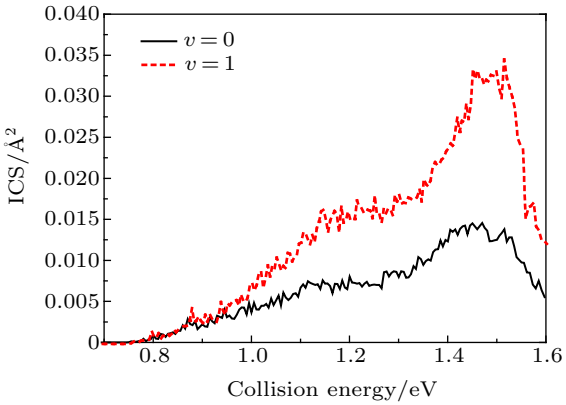


Fig. 4. (color online) Total reaction cross section for the H + $S_2(X^3\Sigma_g^-, v, j = 0)$ reaction for two v values.

3.4. Rate constant

As a very important physical parameter in chemical kinetics, rate constant can influence directly the rapidity of a chemical reaction. In Fig. 5 we display the temperature dependence of thermal rate constant. At about 1000 K it begins to increase until the effective temperature is 4000 K, then it has a trend of decreasing with the temperature. The major reasons for the former phenomenon are two folds. First, the rapid movement of the molecules with the rise of temperature leads to the increase in the reaction probability. Second, the increase in the molecular kinetic energy with the rise in temperature benefits from overcoming the active energy barrier, and gives rise to the increase in thermal rate constant. However, when the effective temperature is above 4000 K, the combined result of the energy dependence of the ICS and the temperature-dependent electronic partition function (10) leads to negative temperature dependence of the H + S_2 thermal rate constant.[37] In addition, our calculated maximum rate constant, 1.02×10^{-14} cm^3·s^{-1} at 4000 K, illustrates that the reaction is slow at ordinary concentration. This result may arise from the fact that the reactant is of a higher activation energy.

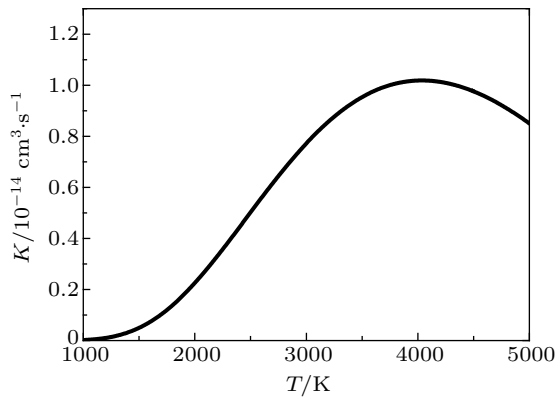


Fig. 5. Temperature dependence of the rate constant for the reaction.

4. Conclusion

In this paper, we have investigated the quantum dynamics of the $H(^2S) + S_2(X^3\Sigma_g^-) \rightarrow SH(X^2\Pi) + S(^3P)$ reaction on an accurate global PES for the ground-state HS_2 (X^2A''). Some dynamical information, such as reaction probabilities, ICS, rate constants, etc., has been provided. The results show that near $E_c = 0.7$ eV, the reaction probabilities have a threshold, and the strong resonance characteristics of the probabilities changing with collision energy are attributed to the existence of the long-lived resonances supported by the deep well. Because the partial wave sum does not wash away all the resonance features, the obtained energy dependence of ICS also shows residual oscillations, which is the typical feature for the well reaction. The calculated rate constant shows not only its negative temperature dependence when $T > 4000$ K, but also the low reactivity of the related reaction for higher activation energy. We expect that these results are probably helpful for further theoretical calculations and can provide some information for the relevant experiments.

Acknowledgments

We thank Prof. Lin Shi-Ying of Shandong University for providing the computational code.

References

[1] Visscher C, Lodders K and Jr B F 2006 *Astrophys. J.* **648** 1181
[2] Farquhar J, Savarino J, Jackson T L and Thiemens M H 2000 *Nature* **404** 50
[3] Bezard B 1983 *Icarus.* **55** 259
[4] Glavas S and Toby S 1975 *J. Phys. Chem.* **79** 779
[5] Sendt K, Jazbec M and Haynes B S 2002 *Proc. Combust. Inst.* **29** 2439
[6] Zhang Y F, Wang M S, Yang C L, Ma M Z, Pang W X and Ma R C 2008 *Chin. Phys. B* **17** 4163
[7] Denis P A 2005 *Chem. Phys. Lett.* **402** 289
[8] Xie D Q, Xu C X, Ho T S, Rabitz H, Lendvay G, Lin S Y and Guo H 2007 *J. Chem. Phys.* **126** 074315
[9] Ma J Y, Guo H, Xie C J, Li A Y and Xie D Q 2011 *Phys. Chem. Chem. Phys.* **13** 8407
[10] Porter G 1950 *Discuss. Farad. Soc.* **9** 60
[11] Cheng B M and Hung W C 1996 *J. Phys. Chem.* **100** 10210
[12] Yamamoto S and Saito S 1994 *Can. J. Phys.* **72** 954
[13] Ashworth S H, Evenson K M and Brown J M 1995 *J. Mol. Spectrosc.* **172** 282
[14] Tanimoto M, Klaus T, Müller H S P and Winnewisser G 2000 *J. Mol. Spectrosc.* **199** 73
[15] Entfellner M and Boesl U 2009 *Phys. Chem. Chem. Phys.* **11** 2657
[16] Ashworth S H and Fink E H 2007 *Mol. Phys.* **105** 715
[17] Peterson K A, Mitrushchenkov A and Francisco J S 2008 *Chem. Phys.* **346** 34
[18] Bajeh M A, Goldfield E M, Hanf A, Kappel C, Meijer A J H M, Volpp H R and Wolfrum J 2001 *J. Phys. Chem. A* **105** 3359
[19] Song Y Z and Varandas A J C 2011 *J. Phys. Chem. A* **115** 5274
[20] Chu T S and Han K L 2005 *J. Phys. Chem. A* **109** 2050
[21] Chu T S, Zhang Y and Han K L 2006 *Int. Rev. Phys. Chem.* **25** 201
[22] Liu X G, Zhang Q G, Zhang Y C, Wang M L and Zhang Z H 2004 *Chin. Phys.* **13** 1013
[23] Althorpe S C and Clary D C 2003 *Annu. Rev. Phys. Chem.* **54** 493
[24] Guo H 2007 *Rev. Comput. Chem.* **25** 285
[25] Gray S K and Kurti G G B 1998 *J. Chem. Phys.* **108** 950
[26] Ledorstier C, Bisseling R H, Cerjan C, Reit M D, Friesner R and Guldberg A 1991 *J. Comput. Phys.* **94** 59
[27] Sun Z P, Lin S Y and Zheng Y J 2011 *J. Chem. Phys.* **135** 234301
[28] Sun Z P, Zhang C F, Lin S Y, Zheng Y J and Meng Q T 2013 *J. Chem. Phys.* **139** 014306
[29] Chu T S and Han K L 2008 *Phys. Chem. Chem. Phys.* **10** 2431
[30] Mandelshtam V A and Taylor H S 1995 *J. Chem. Phys.* **103** 2903
[31] Light J C and Jr T C 2000 *Adv. Chem. Phys.* **114** 263
[32] Lin S Y and Guo H 2006 *Phys. Rev. A* **74** 022703
[33] Meijie A J H M, Goldfield E M, Gray S K and Kurti G G B 1998 *Chem. Phys. Lett.* **293** 270
[34] Bearda R A, VanHemert M C and VanDishoeck E F 1992 *J. Chem. Phys.* **97** 8240
[35] Zhang Z H 1996 *Theory and Applicaiton of Quantum Molecular Dynamics* (NJ: World Scientific) p. 177
[36] Varandas A J C 1995 *Mol. Phys.* **85** 1159
[37] Lin S Y, Guo H, Honvault P, Xu C X and Xie D Q 2008 *J. Chem. Phys.* **128** 014303